DNA METHYLTRANSFERASE 3 (MET3) is regulated by Polycomb Group complex during Arabidopsis endosperm development

Louis Tirot[1] and Pauline E. Jullien[1†]

[1] Institute of Plant Sciences, University of Bern, Bern, Switzerland.

[†]*Corresponding author:* Pauline E. Jullien (pauline.jullien@ips.unibe.ch)

Key message

The DNA METHYLTRANSFERASE MET3 is controlled by Polycomb group complex during endosperm development.

Abstract

Complex epigenetic changes occur during plant reproduction. These regulations ensure the proper transmission of epigenetic information as well as allowing for zygotic totipotency. In *Arabidopsis*, the main DNA methyltransferase is called MET1 and is responsible for methylating cytosine in the CG context. The *Arabidopsis* genome encodes for three additional reproduction-specific homologs of *MET1*, namely *MET2a*, *MET2b* and *MET3.* In this paper, we show that the DNA methyltransferase *MET3* is expressed in the seed endosperm and its expression is further restricted to the chalazal endosperm. *MET3* is biallelically expressed in the endosperm but displays a paternal expression bias. We found that *MET3* expression is regulated by the Polycomb complex proteins FIE and MSI1. Seed development is not impaired in *met3* mutant, and we could not observe significant transcriptional changes in *met3* mutant. Interestingly, we found that *MET3* regulates gene expression in a Polycomb mutant background suggesting a further complexification of the interplay between H3K27me3 and DNA methylation in the seed endosperm.

Keywords

DNA methylation, *Arabidopsis*, endosperm, Polycomb, *MET3*

Introduction

Sexual reproduction in Angiosperm is initiated by a double fertilization event. Fertilization of the haploid egg cell by one of the sperm cells gives rise to the diploid embryo whereas fertilization of the homodiploid central cell gives rise to the triploid endosperm (Berger 2003; Costa et al. 2004). The endosperm represents a nourishing tissue supporting embryo growth and is therefore key for proper seed development. Cell divisions in the endosperm are initiated very rapidly following fertilization. These divisions are initially occurring without cellularization and form a syncytium that will later cellularize (Brown et al. 1999, 2003; Boisnard-Lorig et al. 2001). An additional peculiarity of the endosperm, beyond its triploid syncytial nature, is being the seat of interesting epigenetic phenomena and complex epigenetic regulation.

Endosperm development and cellularization are indeed regulated by the FIS Polycomb group complex known to mediate Histone H3 Lysine 27 tri-methylation, a key silencing epigenetic mark. Some of the key members of the FIS Polycomb group complex (FIS-PcG) are MEA, FIS2, FIE, and MSI1 (Chaudhury et al. 1997; Luo et al. 1999; Kiyosue et al. 1999; Yadegari et al. 2000; Köhler et al. 2003; Guitton et al. 2004). In mutants affecting those genes, the endosperm fails to cellularize, resulting in an arrest of embryo development and eventually seed abortion. Additionally, several genes were found to be imprinted, *i.e.* only one parental allele is expressed whereas the other is epigenetically silent, in the endosperm. This is the case, for example, of genes such as *FIS2*, *FWA*, *MEA* or *PHE1* (Kinoshita et al. 1999, 2004; Luo et al. 2000; Köhler et al. 2005; Jullien et al. 2006). The silencing of those endosperm imprinted genes relies principally on two epigenetic mechanisms: either regulation by the FIS-PcG itself like for *MEA* or *PHE1* or silencing by DNA methylation like for *FWA* and *FIS2* (Jullien and Berger 2009; Gehring 2013; Batista and Köhler 2020). Another epigenetic singularity of the endosperm is of being relatively hypomethylated compared to other plant tissues (Gehring et al. 2009; Hsieh et al. 2009). This hypomethylation is due in part to the activity of a DNA glycosylase called DEMETER (Choi et al. 2002; Gehring et al. 2006; Hsieh et al. 2009) and likely also to the low expression of canonical actors of the DNA methylation pathway (Jullien et al. 2012).

DNA methylation is a key epigenetic mark regulating gene expression and protecting genome integrity by repressing transposons. In plant genomes, DNA methylation is found in three cytosine contexts: CG, CHG and CHH (where H is any base except C). Methylation on these different contexts relies on specific DNA methyltransferases. DNA methylation on CG sites relies on maintenance DNA METHYLTRANSFERASE (MET) where the main ubiquitous enzyme is MET1. DNA methylation on CHG sites relies on CHROMOMETHYLASE3 (CMT3) and an interplay with histone methylation (Lindroth et al. 2001). DNA methylation on CHH site, due to its non-symmetrical nature, relies on the constant *de novo* methylation pathway involving small RNA molecules as well as DOMAIN REARANGED METHYLTRANSFERASE2 (DRM2) (Cao and Jacobsen 2002). In centromeric sequences, CHH methylation also relies on CHROMOMETHYLASE2 (CMT2) (Stroud et al. 2013).

Although we know a lot about the main actors of this pathway, the *Arabidopsis*'s genome encodes multiple copies of DNA methyltransferase genes (4 *METs*, 3 *CMTs* and 3 *DRMs*) some of which might have a more complex or similar function in discreet cell types. For example, *CMT1* (the third CHROMOMETHYLASE encoded by the *Arabidopsis* genome) is principally detected in reproductive tissue (Henikoff and Comai 1998; Klepikova et al. 2016) and the reconstitution of a full-length transcript relies on the splicing out of a transposable element situated in its 13th exon (Yadav et al. 2018). The *DOMAIN REARANGED METHYLTRANSFERASE1* (*DRM1*) seems to also solely play a role in reproductive tissue, where a redundancy between *DRM1* and *DRM2* was observed in the early embryo (Jullien et al. 2012). Similarly, data concerning the potential function of non-canonical *METs* are scarce. *MET2a* and *MET2b* are detected in the central cell, but their function is unknown (Jullien et al. 2012). Nonetheless, correlative evidence suggest *MET2a* might be important to regulate transposon reactivation in wild *Arabidopsis* accessions (Quadrana et al. 2016) and involved in fungal response (Salvador-Guirao et al. 2018).

As mentioned, little is known about the DNA methyltransferase *MET3*. *MET3* is also named *MATERNAL EFFECT EMBRYO ARREST 57* (*MEE57*) as a transposon insertion associated with the *MET3*

77 locus led to an arrest in endosperm development (Pagnussat et al. 2005). *MET3* is also reported to be
78 the sole *MET* expressed in the endosperm (Jullien et al. 2012). Here, we show that *MET3* is specifically
79 expressed in the endosperm in a biallelic fashion with a paternal bias. *MET3* expression is controlled
80 by the FIS-PcG complex. Despite the initial report of a seed arrest phenotype in the *mee57* line, we
81 did not see any seed developmental phenotype in two independent *met3* mutant alleles. Additionally,
82 we could not see major changes in the seed transcriptome of *met3* mutant. Nevertheless, we could
83 see an effect on the seed transcriptome in a *fie* mutant background suggesting that *MET3* might
84 interplay with PcG gene regulation in the developing endosperm.

85 ## *Material and Methods*

86 ### *Plant Materials, Growth Conditions and Genotyping.*

87 The wild-types Col-0 and Gr-1, the *MET3* mutant lines *met3-3* (GABI404F04), *met3-4* (GABI659H03)
88 and PRC2 mutant lines *fie-362* (GABI_362D08) (Bouyer et al. 2011) and *msi1* (SAIL_429_B08) were
89 provided by the Nottingham Arabidopsis Stock Center (NASC). *pMET3:H2B-RFP* line was previously
90 described (Jullien et al. 2012). After sowing, plants were stratified in the dark at 4°C between 2 and 4
91 days. Plants were germinated and grown in growing chambers under long-day conditions (16h light
92 22°C / 8h dark 18°C). For the transmission analysis (Fig. S5a), plants were grown on Murashige and
93 Skoog (MS1/2) media agarose plate in long-day conditions for 12 days before genotyping. Primers for
94 genotyping are listed in Table S1.

95 ### *Microscopy and phenotype observation*

96 DIC seed phenotype and GUS observations were done using a Leica DM2000 as previously described
97 (Jullien et al. 2006). For seed development observation and counting (Fig. 4a) , plants were
98 synchronized by removing all open flowers from the inflorescences. After 6 days, the two first siliques
99 situated above the previously removed flowers were picked for each inflorescence. We refer to this
100 stage as 6 days after synchronization (6 DAS). Siliques were dissected, cleared using chloride hydrate

solution and mounted on a slide for observation. *pMET3:H2B-tdTomato* and *pMET3:H2B-RFP* reporter lines were imaged using a laser scanning confocal microscope (Leica SP5). When necessary, brightness and contrast were uniformly modified by using ImageJ.

Cloning and transformation

pMET3:H2B-tdTomato and *pMET3:H2B-GUS* were generated using the Gateway Cloning System (Invitrogen). All PCR fragments were amplified by PCR using the Phusion High-Fidelity DNA Polymerase (Thermo). Primer sequences used for cloning can be found in Table S1. All plasmids were transformed into wild-type Columbia-0 plants the by floral dipping method (Clough and Bent 1998). At least ten transgenic lines were analyzed per construct, which showed a consistent fluorescence expression pattern. An Illustration of the constructs can be found in Fig. S2a.

RNA extraction, qPCR & RT-PCR

Total RNAs were extracted using RNeasy Plant Minikit (Qiagen). All samples were treated with DNase I (ThermoScientific) at 37°C for 30 minutes. DNAse I was subsequently inactivated by the addition of EDTA and heat treatment (65°C for 10 minutes). First-strand cDNAs were synthesized using between 500 and 1000 ng of DNase treated total RNAs as a template. The RT reaction was performed using either Maxima First Strand cDNA Synthesis Kit (Fig. 1a, Fig. 2a) (ThermoScientific) , containing both oligo-dT and random hexamer primers, or RevertAid RT Reverse Transcription Kit (Fig. 3e, Fig. S4b) (ThermoScientific) , containing only oligo-dT primers. The qPCR reactions were performed with a QuantStudio 5 thermocycler (ThermoScientific) using SYBR green (KAPA SYBR FAST qPCR Master Mix or ORA qPCR Green ROX H Mix). The qPCR mix was prepared according to the manufacturer's protocol. An RNA equivalent of 25 ng of cDNA templates was used for each reaction. The qPCR program was as follow: 95 °C for 3 minutes followed by 45 cycles of 95 °C for 5 seconds and 60 °C for 30 seconds. *ACTIN2* (*AT3G18780*) expression was used to normalize the transcript level in each sample. For each condition, RNA abundance of target genes was calculated from the average of three independent biological replicates with three qPCR technical replicates. Real-time PCR primers used in this study are

listed in Table S1. For the allele-specific RT-PCR (Fig.2a) , cDNAs were amplified for 22 cycles for *ACT2* primers and 35 cycles for *MET3* specific primers. Half of the *MET3* PCR product was digested for 1h30 at 37°C with XbaI restriction enzyme (Sigma-Aldrich). *ACT2* amplification was used as a control.

RNA sequencing and Bioinformatics

Total RNAs were extracted and DNAseI treated as previously mentioned. mRNA libraries were prepared and sequenced by Novogene (https://en.novogene.com/). Bioinformatic analyses were performed on the Galaxy web platform (https://usegalaxy.org) (Afgan et al. 2018). Our Galaxy workflow including the exact parameters and tool versions used can be downloaded on https://usegalaxy.org/u/pej/w/pejrnaseq and be freely reused. Briefly, Paired-end raw mRNA sequencing reads were controlled using FastQC (Galaxy version 0.72) and trimmed using Trimmomatic (Galaxy version 0.36.6) (Andrews 2010; Bolger et al. 2014). Clean reads were aligned to the *Arabidopsis thaliana* TAIR 10 genome assembly using HISAT2 (Galaxy version 2.1.0+galaxy4) (Kim et al. 2015). Aligned sequencing reads were assigned to genomic features using featureCounts (Galaxy version 1.6.2) (Liao et al. 2014). Differential expression was analyzed using DESeq2 default parameters (Galaxy Version 2.11.40.6+galaxy1) (Love et al. 2014). Differentially expressed genes (DEGs) were defined by an absolute logFC > 2 and an FDR < 0.05. Gene ontology (GO) enrichment analysis has been performed on PANTHER (Mi et al. 2019) and visualized using REVIGO (Supek et al. 2011). All plots have been generated using R-studio (www.rstudio.com). Raw data are deposited on the European Nucleotide Archive under reference PRJEB46544 (http://www.ebi.ac.uk/ena/data/view/PRJEB46544).

Results

MET3 is expressed biallelically with a paternal bias in the endosperm

Our previous analysis has shown that *MET3* is expressed in the endosperm of developing *Arabidopsis* seeds (Jullien et al. 2012). However, the detail and exclusivity of its expression pattern remain to be investigated. To get a better characterization of *MET3* expression pattern, we performed

a qPCR of *MET3* transcript in different tissue types of wild-type Col-0 (Fig. 1a). Our result shows that *MET3* is principally expressed in siliques and its expression peaks at 5 Days After Pollination (DAP). These results could be confirmed using publicly available transcriptome datasets (Fig. S1a) (Klepikova et al. 2016). To gain a better spatial and temporal characterization of *MET3* expression, we generated two new transcriptional *MET3* reporter constructs, encompassing 2kb of the *MET3* promoter driving either H2B-tdTomato or H2B-GUS (Fig. S2a). The analysis of the *pMET3:H2B-GUS* in different plant tissues confirmed the specificity of *MET3* expression to the seed endosperm (Fig. S1b-d). To characterize in detail the temporal expression of *MET3* in the endosperm, we performed confocal microscopy on the *pMET3:H2B-tdTomato* lines at different stages of seed development. We could detect *pMET3:H2B-tdTomato* expression from as early as the four nuclei stage endosperm (Fig. 1b). *pMET3:H2B-tdTomato* remains express throughout the endosperm (Fig. 1c) until the globular stage of embryo development where its expression starts to be higher in the chalazal endosperm and chalazal cyst (Fig. 1d). At later stages, *pMET3:H2B-tdTomato* expression is limited to the chalazal endosperm and chalazal cyst (Fig. 1e). From 7 DAP, *pMET3:H2B-tdTomato* expression can no longer be detected. A similar expression pattern was observed with *pMET3:H2B-GUS* (Fig. S2b) and *pMET3:H2B-RFP* (Fig. S2c) as well as online transcriptomic data (Fig. S2d) (Belmonte et al. 2013). MET3 protein expression and localization could not be determined as we, so far, failed in expressing a fluorescently tagged MET3 protein in *Arabidopsis* (LT personal communication).

Such endosperm expression pattern is common in imprinted genes, like *FWA*, *FIS2*, *MEA* or *PHE1* (Kinoshita et al. 1999, 2004; Köhler et al. 2005; Jullien et al. 2006). In order to examine if *MET3* is biallelically or mono-allelically expressed, we performed allele-specific RT-PCR. We are making use of a Short Nucleotide Polymorphism (SNP) consisting of a substitution from a C to a T within *MET3* 9th exon in the Gr-1 ecotype which is abolishing a XbaI restriction site present in Col-0. We did reciprocal crosses using Col-0 and Gr-1 ecotypes and analyzed *MET3* parental expression at 5 DAP following XbaI digestion (Fig. 2a). We could observe, for both reciprocal crosses, bands corresponding to *MET3* transcript from Col-0 (505 and 329 bp) and from Gr-1 (834 bp) with a bias toward the paternal allele.

This result shows that *MET3* is expressed from both maternal and paternal allele but displays a paternal bias of expression. *MET3* paternally biased expression was also observed using the *pMET3:H2B-RFP* transgene at 1 DAP (Fig.2b). Taking together our results shows that *MET3* expression is biallelic with a paternal bias and confined to the endosperm. *MET3* expression, initially throughout the endosperm, becomes restricted to the chalazal pole at later stages.

MET3 expression is regulated by Polycomb group proteins

Beyond imprinted genes, *MET3* expression pattern is reminiscent of the expression of genes controlled by the endosperm FIS Polycomb group complex (PcG) composed of FIE, MSI1, FIS2 and MEA (Guitton et al. 2004). To investigate if *MET3* could be regulated by PcG, we introgressed a *MET3* transcriptional reporter into *fie* and *msi1* mutant background (Fig. 3a-d). We could observe increased *pMET3:H2B-RFP* reporter expression in 49% of the seeds (n=249) in *fie/+* mutant and 44% (n=240) in *msi1/+* mutant background characteristic of the maternal gametophytic effect of those mutations (Fig. 3d). In *msi1* and *fie* mutants, *pMET3:H2B-RFP* expression is higher and observed throughout the endosperm (Fig. 3b-c) whereas at the same developmental stage the expression of *pMET3:H2B-RFP* is already restricted to the chalazal pole in wild-type seeds (Fig. 3a). In order to confirm that the regulation of *MET3* by *MSI1* and *FIE* was not only restricted to our transgene, we performed a RT-qPCR of *MET3* expression in wild-type and mutant selected seeds at 10 DAP (Fig. 3e). We could observe a clear upregulation of *MET3* expression in both *fie* and *msi1* seeds compare to wild-type seeds (t-test p-value of 0.0543 and 0.0114 respectively). Using publicly available data, we could see that the upregulation of *MET3* is also observed in other PcG mutants (Fig. S3a-b). *MET3* upregulation was observed in silique samples of *clf* mutant (Fig. S3a) (Liu et al. 2016) and in *fis2* seeds (Fig. S3b) (Weinhofer et al. 2010).

Subsequently, we wanted to know if the effect of the PcG complex was direct or indirect. PcG complexes are known to repress gene expression by tri-methylating the Lysine 27 of the Histone H3 tail (H3K27me3) inducing a closed chromatin state at the targeted loci. We, therefore, analyzed

available H3K27me3 genome-wide Chromatin Immunoprecipitation (ChIP) data. We could see that the *MET3* locus is covered by H3K27me3 in *Arabidopsis* seedling samples (Fig. 3f) (Zhang et al. 2007). Additionally, using the RepMap2020 tool (Chèneby et al. 2020) , we could observe H3K27me3 on the *MET3* locus in several independent ChIP experiments including some performed on endosperm tissue (Fig. S3c). We conclude that *MET3* expression is directly repressed by PcG complex induced H3K27me3 in the endosperm.

MET3 does not affect seed development

Considering that *MET3* is specifically expressed in the developing endosperm during seed development, we then ask if *MET3* function influences seed and/or endosperm development. We characterized two mutant alleles from the GABI collection: *met3-3* (GABI_404F04) and *met3-4* (GABI_659H03) (Fig. S4a). The mutations are located on the 10th and the 2nd exon respectively and are expected to abolish *MET3* function. To confirm the downregulation of *MET3* in the mutants, we performed RT-qPCR. We could observe that *MET3* is downregulated in both mutant alleles (Fig. S4b). To investigate if the *met3* mutation could result in seed lethality we first investigated the presence of aborted seeds at the green seed stage (~12DAP). We could not see any significant seed abortion in both *met3-3* and *met3-4* alleles (Fig. S5b). To further confirm the absence of defects, we analyzed the transmission rate of the *met3* mutations in *met3-3/+* and *met3-4/+* selfed progeny. We could not observe any segregation distortion from the Mendelian ratio (Fig. S5a). Mutations affecting the main *Arabidopsis* DNA methyltransferase *MET1* display variation in seed size. We, therefore, investigated if *met3* mutants would display a seed size phenotype. We could not see any significant variation in seed size using both *met3* alleles (Fig. S5c-d). We conclude that *MET3* mutation does not severely impair seed development. Additionally, *met1* mutant are known to display increased developmental defect through generation (Mathieu et al. 2007). To assess potential transgenerational effect of the *met3* mutation we have maintained *met3* homozygotes mutants for five generations. However, we could not observe such increased developmental phenotype with *met3* mutants after five generation of inbreeding (*met3*^{G5}) (Fig. S5e-g). The *met3*^{G5} did not show difference when compared to wild-type

either in term of rosette size (Fig. S5f) nor flowering time (Fig. S5g). We conclude that *MET3* mutations do not severely impair seed development and do not accumulate transgenerational developmental defects.

As shown above, *MET3* expression is regulated by PcG complex in the endosperm, we then analyzed if *MET3* mutation could influence the PcG *fie* mutant phenotype. To answer this question, we generated *fie*/+;*met3-3* and *fie*/+;*met3-4* double mutants and analyzed their seed development phenotype using DIC (Fig. 4a-f). In order to minimize the stress to the plant due to handling during emasculation and crossing, we used "synchronized seeds". In practice, we remove the open flowers of the day, and we wait an x number of days before collecting two siliques above our cutting. This is allowing us to have age synchronized siliques without the physical disturbance of emasculation/pollination and is, therefore, closer to normal growth and fertilization. We are using the term Day After Synchronization (DAS). To our experience, 6 DAS is corresponding to around 4-5DAP. At 6 DAS, we could not see any delay in embryo development and endosperm cellularization comparing Col-0 to *met3-3* and *met3-4* mutants (Fig. 4a-c, 4g-h). In *fie*/+, we could clearly see the delayed endosperm cellularization characteristic of FIS-PcG mutants (Fig. 4d-f and h) (56% n=407) (Ohad et al. 1999; Sørensen et al. 2001). In the double mutants, we could not see variations in the quantification of the *fie*/+ phenotype for both embryo development (Fig. 4g) and endosperm cellularization (Fig. 4h). We conclude that *MET3* mutations do not influence *fie* mutant seed phenotype.

Effect of MET3 mutation on the seed transcriptome

In order to investigate the potential effect of *met3* mutation on the seed transcriptome, we performed a mRNA deep sequencing experiment of 3 DAP (Fig. S6) and 10 DAS (Fig. 5a) seeds (*i.e.* seeds attached to the septum). We then compared the seed transcriptome of *met3* seeds to wild-type seeds. At 3 DAP, we could only detect one differentially expressed gene: *ESM1* (*AT3G14210*). *ESM1* was up-regulated in both *met3-3* and *met3-4* mutant seeds (Fig. S6a-b). At 10 DAS, we could also only

see very minor changes to the seed transcriptome (Fig. 5a). We could identify only 16 differentially expressed genes with an absolute logFC>2 and FDR<0.05. These results show that reminiscent of the absence of seed phenotype in *met3* mutants, the seed transcriptome is also mostly unaffected by the *met3* mutation. As *MET3* expression is regulated by the FIS-PcG complex in the endosperm, we then ask if *MET3* mutation could influence the *fie* transcriptome. We, therefore, sequenced the transcriptome of 10 DAS seeds where we selected for *fie* mutant seeds under the dissecting microscope (white seeds). We compared the transcriptome of *fie* seeds to the transcriptome of *fie;met3-3* double mutant seeds. We could observe 87 differentially expressed genes (DEG) with an absolute logFC>2 and FDR<0.05 (Fig 5b). A Goterm enrichment analysis revealed that these genes are enriched for genes involved in pectin metabolism (GO:0045490, FDR=4.46E-10; GO:0045488, FDR=6.59E-09) and cell-wall related processes (GO:0042545, FDR= 8.97E-09; GO:0071555, FDR=4.87E-10, GO:0071554, FDR=5.67E-08) (Fig. 5c and Table S2). We then analyzed if among these 87 DEGs some are also modified in *fie* mutant compared to wild-type. We could find that a large proportion of either *met3* DEGs (Col vs *met3*, 11/16) and *met3;fie* DEGs (*fie* versus *met3fie*, 44/87) are miss-regulated in *fie* mutant seeds (Fig. 5d). We conclude that the *met3* mutation does not drastically change the seed transcriptome, but a set of genes are miss-regulated by both *met3 and fie mutants*.

Discussion

Our study highlights an additional connection between DNA Methylation pathways and Polycomb group H3K27 tri-methylation in the seed endosperm via the regulation of *MET3* by the FIS-PcG complex. *MET3* is specifically expressed in the endosperm, and its expression becomes restricted to the chalazal pole at later stages of endosperm development. In our study, using two independent insertion lines, *met3-3* and *met3-4*, we could not observe any major seed developmental phenotype. Both mutants show a significant decrease in *MET3* expression by qPCR suggesting they both represent knockout mutants. It was previously documented that a mutation affecting *MET3* named *mee57* displayed a strong seed developmental phenotype (Pagnussat et al. 2005). The *mee57* mutation shows

277 an early maternal embryo and endosperm arrest. The discrepancy between our lines and the
278 previously published *mee57* could have several causes: the mutagenesis method used (T-DNA versus
279 transposition) , the presence of additional genetic modifications, or a difference between the two
280 ecotypes used, Columbia-0 in our case and Landsberg for *mee57*. If the latter is true, *MET3* function
281 could vary between different *Arabidopsis* accessions.

282 In this work, we show that repression of *MET3* expression at later stages of endosperm
283 development is linked to the direct action of the FIS-PcG complex on the *MET3* locus. *MET3* is over-
284 expressed in PcG mutant seeds, such as *fie* and *msi1* mutant seeds. Interestingly, it was previously
285 shown that *fie* mutant endosperm display higher CG methylation compared to wild-type endosperm
286 and lower CHG and CHH (Ibarra et al. 2012). This increased CG methylation in *fie* mutant seems to be
287 restricted to the endosperm as it is not observed in *fie* seedling or *fie* embryo methylome (Bouyer et
288 al. 2017). We propose that higher expression of *MET3* in the *fie* endosperm could be the cause for the
289 increase in CG methylation specifically in the endosperm. Indeed, in our study, we could not observe
290 any change in *MET3* tissue expression pattern in PcG mutants but the increased expression is still
291 restricted to the endosperm. In further studies, the Investigation of the endosperm methylome in
292 *met3* and *met3;fie* mutants will allow to test this hypothesis. Additionally, further experiments are
293 required to determine if MET3 is a functional DNA methyltransferase.

294 As we previously mentioned, *MET3* function could vary in between wild *Arabidopsis* accessions.
295 Similarly, to CMT1, several SNPs can be found at the *MET3* locus in-between different ecotypes
296 suggesting that *MET3* might not be fully functional in all of them. Additionally, looking closer at the
297 *MET3* locus, we could detect the presence of a Class 2 DNA transposon (*AT4TE34810*) situated in the
298 third intron of the *MET3* gene. In addition to PcG regulation, *MET3* expression and possibly function
299 could be influenced by the presence or regulation of *AT4TE34810* like it is the case for *CMT1* transcript
300 (Yadav et al. 2018). The study of *MET3* function and imprint in different accession could reveal more
301 about its function in natural growth conditions. One hint of *MET3* potential function in Columbia-0

302 came from the study of methylome stability across several generations (Becker et al. 2011). In this
303 study, methylome stability was investigated in several Col-0 selfed lineages (30 generations). The line
304 accumulating the most methylation polymorphisms had concomitantly acquired a SNP in the *MET3*
305 gene. It was therefore suggested that *MET3* could be the cause of such methylome instability (Becker
306 et al. 2011; Schmitz and Ecker 2012). Analyzing the methylome of selfed *met3* mutants after 30
307 generations would allow to test this hypothesis. If true and taking into account the endosperm
308 specificity of *MET3* expression, it would indicate that the endosperm methylome influences the
309 embryonic methylome, a hypothesis that has stimulated a lot of interest over the last 10 years but
310 remains to be demonstrated.

311 ## *Acknowledgments*

312 We would like to thank the following people for their help: Jasmine Sekulovski for support
313 concerning plant growth, Diane Bonnet for technical support. We thank Mathieu Ingouff and Diane
314 Bonnet for critical reading of the manuscript.

315 ## *Funding*

316 PEJ and LT are supported by an SNF professorship grant (no.163946) attributed to PEJ.

317 ## *Author contributions*

318 PEJ conceived the study. LT performed the experiments. LT and PEJ analyzed the data. PEJ wrote
319 the manuscript with the help of LT.

320 ## *Conflicts of interest*

321 Authors state that there is no conflict of interest.

322

References

Afgan E, Baker D, Batut B, et al (2018) The Galaxy platform for accessible, reproducible and collaborative biomedical analyses: 2018 update. Nucleic Acids Res 46:W537–W544. https://doi.org/10.1093/nar/gky379

Andrews S (2010) FastQC: a quality control tool for high throughput sequence data.

Batista RA, Köhler C (2020) Genomic imprinting in plants-revisiting existing models. Genes Dev 34:24–36. https://doi.org/10.1101/gad.332924.119

Becker C, Hagmann J, Müller J, et al (2011) Spontaneous epigenetic variation in the Arabidopsis thaliana methylome. Nature 480:245–9. https://doi.org/10.1038/nature10555

Belmonte MF, Kirkbride RC, Stone SL, et al (2013) Comprehensive developmental profiles of gene activity in regions and subregions of the Arabidopsis seed. Proc Natl Acad Sci 110:E435–E444. https://doi.org/10.1073/pnas.1222061110

Berger F (2003) Endosperm: The crossroad of seed development. Curr Opin Plant Biol 6:42–50. https://doi.org/10.1016/S1369526602000043

Boisnard-Lorig C, Colon-Carmona A, Bauch M, et al (2001) Dynamic analyses of the expression of the HISTONE::YFP fusion protein in arabidopsis show that syncytial endosperm is divided in mitotic domains. Plant Cell 13:495–509

Bolger AM, Lohse M, Usadel B (2014) Trimmomatic: A flexible trimmer for Illumina sequence data. Bioinformatics 30:2114–2120. https://doi.org/10.1093/bioinformatics/btu170

Bouyer D, Kramdi A, Kassam M, et al (2017) DNA methylation dynamics during early plant life. Genome Biol 18:179. https://doi.org/10.1186/s13059-017-1313-0

Bouyer D, Roudier F, Heese M, et al (2011) Polycomb repressive complex 2 controls the embryo-to-

345 seedling phase transition. PLoS Genet 7:. https://doi.org/10.1371/journal.pgen.1002014

346 Brown RC, Lemmon BE, Nguyen H (2003) Events during the first four rounds of mitosis establish
347 three developmental domains in the syncytial endosperm of Arabidopsis thaliana. Protoplasma
348 222:167–74. https://doi.org/10.1007/s00709-003-0010-x

349 Brown RC, Lemmon BE, Nguyen H, Olsen OA (1999) Development of endosperm in Arabidopsis
350 thaliana. Sex Plant Reprod 12:32–42. https://doi.org/10.1007/s004970050169

351 Cao X, Jacobsen SE (2002) Locus-specific control of asymmetric and CpNpG methylation by the DRM
352 and CMT3 methyltransferase genes. Proc Natl Acad Sci U S A 99:16491–16498.
353 https://doi.org/10.1073/pnas.162371599

354 Chaudhury a M, Ming L, Miller C, et al (1997) Fertilization-independent seed development in
355 Arabidopsis thaliana. Proc Natl Acad Sci U S A 94:4223–8

356 Chèneby J, Ménétrier Z, Mestdagh M, et al (2020) ReMap 2020: A database of regulatory regions
357 from an integrative analysis of Human and Arabidopsis DNA-binding sequencing experiments.
358 Nucleic Acids Res 48:D180–D188. https://doi.org/10.1093/nar/gkz945

359 Choi Y, Gehring M, Johnson L, et al (2002) DEMETER, a DNA glycosylase domain protein, is required
360 for endosperm gene imprinting and seed viability in arabidopsis. Cell 110:33–42

361 Clough SJ, Bent AF (1998) Floral dip: A simplified method for Agrobacterium-mediated
362 transformation of *Arabidopsis thaliana*. Plant J 16:735–743. https://doi.org/10.1046/j.1365-
363 313X.1998.00343.x

364 Costa LM, Gutièrrez-Marcos JF, Dickinson HG (2004) More than a yolk: The short life and complex
365 times of the plant endosperm. Trends Plant Sci 9:507–514.
366 https://doi.org/10.1016/j.tplants.2004.08.007

Gehring M (2013) Genomic imprinting: insights from plants. Annu Rev Genet 47:187–208. https://doi.org/10.1146/annurev-genet-110711-155527

Gehring M, Bubb KL, Henikoff S (2009) Extensive demethylation of repetitive elements during seed development underlies gene imprinting. Science (80-) 324:1447–51. https://doi.org/10.1126/science.1171609

Gehring M, Huh JH, Hsieh TF, et al (2006) DEMETER DNA Glycosylase Establishes MEDEA Polycomb Gene Self-Imprinting by Allele-Specific Demethylation. Cell 124:495–506. https://doi.org/10.1016/j.cell.2005.12.034

Guitton A, Page DR, Chambrier P, et al (2004) Identification of new members of Fertilisation Independent Seed Polycomb Group pathway involved in the control of seed development in Arabidopsis thaliana. Development 2971–2981. https://doi.org/10.1242/dev.01168

Henikoff S, Comai L (1998) A DNA Methyltransferase Homolog With a Chromodomain Exists in Multiple Polymorphic Forms in Arabidopsis. Genetics 149:307–318

Hsieh TT-F, Ibarra CA, Silva P, et al (2009) Genome-wide demethylation of Arabidopsis endosperm. Science (80-) 324:1451–1454. https://doi.org/10.1126/science.1172417

Ibarra CA, Feng X, Schoft VK, et al (2012) Active DNA Demethylation in Plant Companion Cells Reinforces Transposon Methylation in Gametes. Science (80-) 337:1360–1364. https://doi.org/10.1126/science.1224839

Jullien PE, Berger F (2009) Gamete-specific epigenetic mechanisms shape genomic imprinting. Curr Opin Plant Biol 12:637–642. https://doi.org/10.1016/j.pbi.2009.07.004

Jullien PE, Kinoshita T, Ohad N, Berger F (2006) Maintenance of DNA Methylation during the Arabidopsis Life Cycle Is Essential for Parental Imprinting. Plant Cell 18:1360–1372.

https://doi.org/10.1105/tpc.106.041178.1

Jullien PE, Susaki D, Yelagandula R, et al (2012) DNA methylation dynamics during sexual reproduction in Arabidopsis thaliana. Curr Biol 22:1825–1830. https://doi.org/10.1016/j.cub.2012.07.061

Kim D, Langmead B, Salzberg SL (2015) HISAT: A fast spliced aligner with low memory requirements. Nat Methods 12:357–360. https://doi.org/10.1038/nmeth.3317

Kinoshita T, Miura A, Choi Y, et al (2004) One-Way Control of FWA Imprinting in Arabidopsis Endosperm by DNA Methylation. Science (80-) 303:521–523. https://doi.org/10.1126/science.1089835

Kinoshita T, Yadegari R, Harada JJ, et al (1999) Imprinting of the MEDEA polycomb gene in the Arabidopsis endosperm. Plant Cell 11:1945–52

Kiyosue T, Ohad N, Yadegari R, et al (1999) Control of fertilization-independent endosperm development by the MEDEA polycomb gene in Arabidopsis. Proc Natl Acad Sci 96:4186–4191. https://doi.org/10.1073/pnas.96.7.4186

Klepikova A V., Kasianov AS, Gerasimov ES, et al (2016) A high resolution map of the Arabidopsis thaliana developmental transcriptome based on RNA-seq profiling. Plant J 88:1058–1070. https://doi.org/10.1111/tpj.13312

Köhler C, Hennig L, Bouveret R, et al (2003) Arabidopsis MSI1 is a component of the MEA/FIE Polycomb group complex and required for seed development. EMBO J 22:4804–14. https://doi.org/10.1093/emboj/cdg444

Köhler C, Page DR, Gagliardini V, Grossniklaus U (2005) The Arabidopsis thaliana MEDEA Polycomb group protein controls expression of PHERES1 by parental imprinting. Nat Genet 37:28–30.

411 https://doi.org/10.1038/ng1495

412 Liao Y, Smyth GK, Shi W (2014) FeatureCounts: An efficient general purpose program for assigning
413 sequence reads to genomic features. Bioinformatics 30:923–930.
414 https://doi.org/10.1093/bioinformatics/btt656

415 Lindroth a M, Cao X, Jackson JP, et al (2001) Requirement of CHROMOMETHYLASE3 for maintenance
416 of CpXpG methylation. Science 292:2077–80. https://doi.org/10.1126/science.1059745

417 Liu J, Deng S, Wang H, et al (2016) CURLY LEAF regulates gene sets coordinating seed size and lipid
418 biosynthesis. Plant Physiol 171:424–436. https://doi.org/10.1104/pp.15.01335

419 Love MI, Huber W, Anders S (2014) Moderated estimation of fold change and dispersion for RNA-Seq
420 data with DESeq2. bioRxiv 1–21. https://doi.org/10.1101/002832

421 Luo M, Bilodeau P, Dennis ES, et al (2000) Expression and parent-of-origin effects for FIS2, MEA, and
422 FIE in the endosperm and embryo of developing Arabidopsisseeds. PNAS.
423 https://doi.org/10.1073/pnas.170292997

424 Luo M, Bilodeau P, Koltunow a, et al (1999) Genes controlling fertilization-independent seed
425 development in Arabidopsis thaliana. Proc Natl Acad Sci U S A 96:296–301

426 Mathieu O, Reinders J, Caikovski M, et al (2007) Transgenerational stability of the Arabidopsis
427 epigenome is coordinated by CG methylation. Cell 130:851–862.
428 https://doi.org/10.1016/j.cell.2007.07.007

429 Mi H, Muruganujan A, Huang X, et al (2019) Protocol Update for large-scale genome and gene
430 function analysis with the PANTHER classification system (v.14.0). Nat Protoc 14:703–721.
431 https://doi.org/10.1038/s41596-019-0128-8

432 Ohad N, Yadegari R, Margossian L, et al (1999) Mutations in FIE, a WD polycomb group gene, allow

433 endosperm development without fertilization. Plant Cell 11:407–415.
434 https://doi.org/10.1105/tpc.11.3.407

435 Pagnussat GC, Yu HJ, Ngo QA, et al (2005) Genetic and molecular identification of genes required for
436 female gametophyte development and function in Arabidopsis. Development 132:603–614.
437 https://doi.org/10.1242/dev.01595

438 Quadrana L, Silveira AB, Mayhew GF, et al (2016) The Arabidopsis thaliana mobilome and its impact
439 at the species level. Elife 5:1–25. https://doi.org/10.7554/eLife.15716

440 Salvador-Guirao R, Baldrich P, Weigel D, et al (2018) The MicroRNA miR773 Is Involved in the
441 *Arabidopsis* Immune Response to Fungal Pathogens. Mol Plant-Microbe Interact 31:249–259.
442 https://doi.org/10.1094/MPMI-05-17-0108-R

443 Schmitz RJ, Ecker JR (2012) Epigenetic and epigenomic variation in Arabidopsis thaliana. Trends Plant
444 Sci 17:149–154. https://doi.org/10.1016/j.tplants.2012.01.001

445 Sørensen MB, Chaudhury AM, Robert H, et al (2001) Polycomb group genes control pattern
446 formation in plant seed. Curr Biol 11:277–281

447 Stroud H, Do T, Du J, et al (2013) Non-CG methylation patterns shape the epigenetic landscape in
448 Arabidopsis. Nat Struct Mol Biol 21:64–72. https://doi.org/10.1038/nsmb.2735

449 Supek F, Bošnjak M, Škunca N, Šmuc T (2011) Revigo summarizes and visualizes long lists of gene
450 ontology terms. PLoS One 6:. https://doi.org/10.1371/journal.pone.0021800

451 Weinhofer I, Hehenberger E, Roszak P, et al (2010) H3K27me3 Profiling of the Endosperm Implies
452 Exclusion of Polycomb Group Protein Targeting by DNA Methylation. PLoS Genet 6:e1001152.
453 https://doi.org/10.1371/journal.pgen.1001152

454 Winter D, Vinegar B, Nahal H, et al (2007) An “electronic fluorescent pictograph” Browser for

455 exploring and analyzing large-scale biological data sets. PLoS One 2:1–12.
456 https://doi.org/10.1371/journal.pone.0000718

457 Yadav NS, Khadka J, Domb K, et al (2018) CMT3 and SUVH4/KYP silence the exonic Evelknievel
458 retroelement to allow for reconstitution of CMT1 mRNA 06 Biological Sciences 0604 Genetics.
459 Epigenetics and Chromatin 11:1–12. https://doi.org/10.1186/s13072-018-0240-y

460 Yadegari R, Kinoshita T, Lotan O, et al (2000) Mutations in the FIE and MEA genes that encode
461 interacting polycomb proteins cause parent-of-origin effects on seed development by distinct
462 mechanisms. Plant Cell 12:2367–2382

463 Zhang X, Clarenz O, Cokus S, et al (2007) Whole-genome analysis of histone H3 lysine 27
464 trimethylation in Arabidopsis. PLoS Biol 5:e129. https://doi.org/10.1371/journal.pbio.0050129

465

466

Figure legends

Figure 1. MET3 expression pattern

(a) *MET3* expression measured by RT-qPCR. DAP = Day After Pollination. The histogram displays the mean, and each dot represents a biological replicate. *ACT2* is used as a normalizer. RQ = Relative Quantification (b-e) Single-plan Confocal images representing the expression of *pMET3:H2B-tdTomato* construct in *Arabidopsis* 1 Day After Synchronization (DAS) seed (b), 2 DAS seed (c), 3 DAS (d) and 5 DAS (e). cze = chalazal endosperm, endo = endosperm nuclei. Scale bars represent 25µm.

Figure 2. MET3 is biallelically expressed with a paternal bias

(a) Allele specific RT-PCR of *MET3* parental expression in 5DAP silique samples. The *XbaI* restriction enzyme digests the Col-0 *MET3* transcript but not the Gr-1 transcript. *ACT2* is used as loading control. (b) Single-plan confocal images of *pMET3:H2B-RFP* parental expression in the endosperm of 1 DAP seeds. endo = endosperm nuclei. Scale bars represent 25µm. ♂ symbol indicates the genotype of the male parent while ♀ indicates the genotype of the female parent.

Figure 3. MET3 expression is controlled by FIE and MSI1 Polycomb proteins

(a-c) Confocal images representing the expression of *pMET3:H2B-RFP* construct in *Arabidopsis* wildtype (a), *fie* (b) and *msi1* (c) selfed seeds at 5 days after pollination (DAP). Scale bars represent 50 µm. (d) Proportion of seeds with high RFP signal in the endosperm at 5DAP in wild-type, *fie* and *msi1* mutants. Grey bars represent the seeds with a restricted RFP expression to the chalazal endosperm (as illustrated in (a)). Black bars represent the seeds with ectopic expression of *pMET3:H2B-RFP* throughout the endosperm (as illustrated in (b-c)). (e) *MET3* expression measured by RT-qPCR in 10 DAP selected seeds of wild-type, *fie* and *msi1*. The histogram displays the mean, and each dot represents a biological replicate. *ACT2* is used as a normalizer. (f) Snapshot showing that the *MET3* locus contains H3K27me3 and LHP1 but no H3K4me1, H3K4me2, H3K4me3 and H3K9me2 in seedlings. Data from http://epigenomics.mcdb.ucla.edu/H3K27m3/ (Zhang et al. 2007).

491 *Figure 4. MET3 does not influence fie phenotype*

492 (a-f) Seed developmental phenotype observed after clearing by Difference Interference Contrast (DIC)
493 of wild-type (a), *met3-3* (b), *met3-4* (c), *fie/+* (d), *met3-3;fie/+* (e) and *met3-4;fie/+* (f) at 6 days after
494 synchronization (DAS). Scale bars represent 50 µm. (g-h) Quantification of the embryo developmental
495 stages (g) and endosperm cellularization (h) in wild-type, *met3-3*, *met3-4*, *fie/+*, *met3-3;fie/+* and
496 *met3-4;fie/+* at 6 DAS. mce = micropylar endosperm.

497 *Figure 5. Transcriptome of met3 and met3;fie mutant seeds*

498 (a-b) Volcano plot depicting differentially expressed genes (DEGs) comparing Col-0 to *met3-3* (a) and
499 *fie* to *met3-3;fie* in 10 DAS seeds (b). Red dots represent up-regulated DEGs and blue dots represent
500 down-regulated DEGs. The top 10 DEGs are annotated. We use a threshold of [absolute logFC > 2,
501 FDR < 0.05]. (c) GO term analysis for the 87 DEGs obtained with the *fie vs met3-3;fie* contrast. (d)
502 Venn diagram showing the overlapping DEGs between the different contrasts.

503 *Figure S1. MET3 is only expressed in seeds*

504 (a) Snapshot of the *MET3* expression pattern obtained from ebar using the data from Klepikova *et al.*
505 (Winter et al. 2007; Klepikova et al. 2016)(b-d) The absence of *pMET3:H2B-GUS* expression observed
506 in *Arabidopsis* seedling (b), stamen (c) and ovule (d).

507 *Figure S2. MET3 reporters and expression*

508 (a) Representation of *pMET3:H2B-GUS*, *pMET3:H2B-tdTomato* and *pMET3:H2B-RFP*. (b) *pMET3:H2B-*
509 *GUS* expression observed in 1 DAP and 3 DAP seeds. (c) *pMET3:H2B-RFP* expression observed in 1 DAP
510 and 3 DAP seeds. Scale bars represent 50 µm. (d) Snapshot of expression data from LCM dissected
511 seeds from http://seedgenenetwork.net/plotprobe?name=254720_at (Belmonte et al. 2013).

512 *Figure S3. MET3 regulation by Polycomb group*

513 (a) *MET3* expression from an RNA-seq experiment in inflorescence, root, shoot and siliques from wild-
514 type plants and *clf28* mutant plants, data from Liu *et al* 2016 (Liu et al. 2016). (b) *MET3* expression

515 from transcriptomic data obtained from 3 DAP seeds using MicroArray comparing wild-type to *fis2-1*
516 endosperm, data from Weinhofer *et al* 2010 (Weinhofer et al. 2010). (c) Snapshot of H3K27me3 ChIP
517 data from several tissues including endosperm (colored in blue), flowers (colored in yellow) and
518 various sporophytic (colored in green). Green line represent the presence of ChIP peaks of H3K27me3.
519 Data from ReMap (Chèneby et al. 2020).

520 *Figure S4. Characterization of MET3 mutants*

521 (a) Representation of the *MET3* locus. Blue triangles are representing the T-DNA insertion site of both
522 *met3-3* (GABI_404F04) and *met3-4* (GABI_659H03) (b) *MET3* expression measured by RT-qPCR in Col-
523 0 and *met3* mutants seeds at 3DAP. The histogram displays the mean, and each dot represents a
524 biological replicate. *ACT2* is used as a normalizer. 2 stars indicate a p value <0.01.

525 *Figure S5. MET3 mutants do not show developmental defect*

526 (a) *met3* mutants transmission in self progeny. +/+ represent wild-type, +/- heterozygotes and -/-
527 homozygotes plants for the mutations. (b) Percentage of seed abortion in Col-0 and *met3* mutants
528 (*met3-3* and *met3-4*) siliques. (c) Seed size measurement for Col-0 and *met3* mutants dry seeds. No
529 significant differences observed. (d) Pictures of Col-0 and *met3* mutants dry seeds. The scale bars
530 represent 1 mm. (e) Pictures of Col-0 and *met3* mutants rosette at first (top panel) and fifth generation
531 (bottom panel). The scale bars represent 1 cm. (f) Rosette area measurement in mm^2 of Col and *met3*
532 mutants at fifth generation. n=12. (g) Flowering time (number of days between transplanting and
533 bolting) of Col and *met3* mutants at fifth generation. n=12.

534

535 *Figure S6. Transcriptome of met3 mutant seeds at 3DAP*

536 (a-b) Volcano plot depicting one differentially expressed gene comparing Col-0 to *met3-3* (a) and
537 *met3-4 (b)* at 3DAP.

538

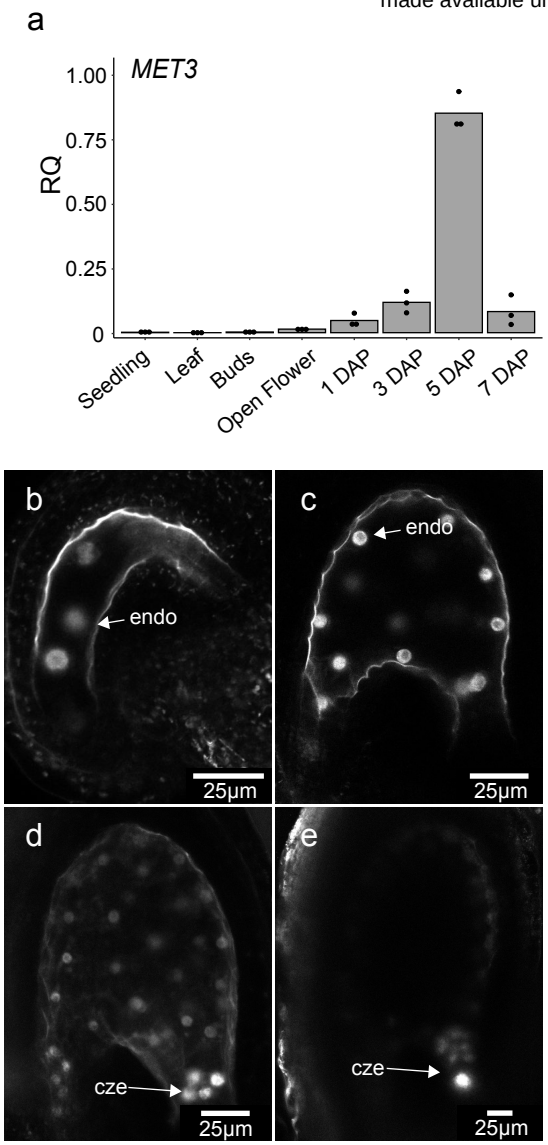

Figure 1. *MET3* expression pattern

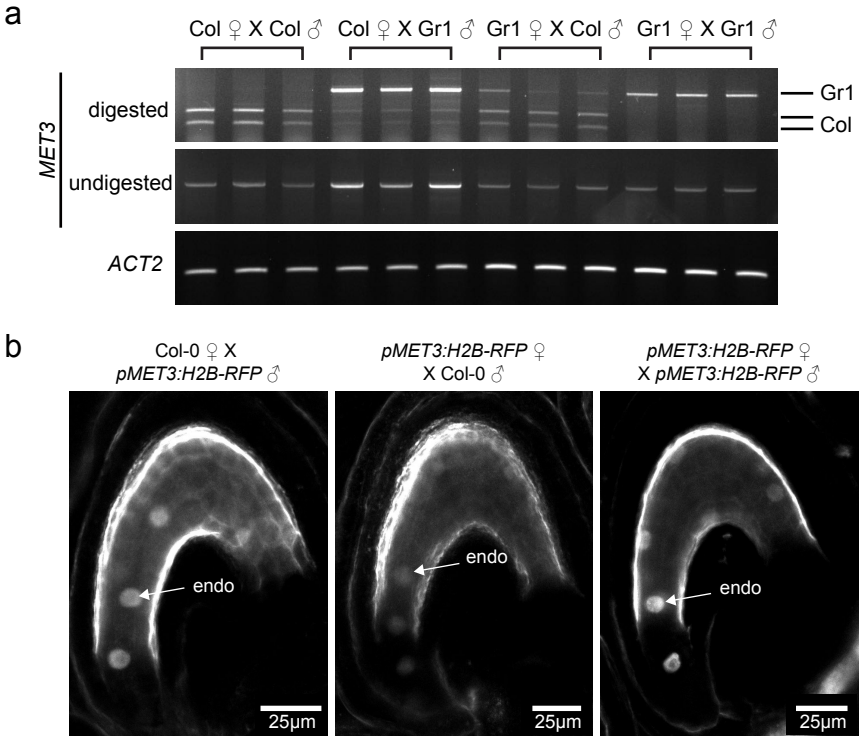

Figure 2. *MET3* is biallelically expressed with a paternal bias

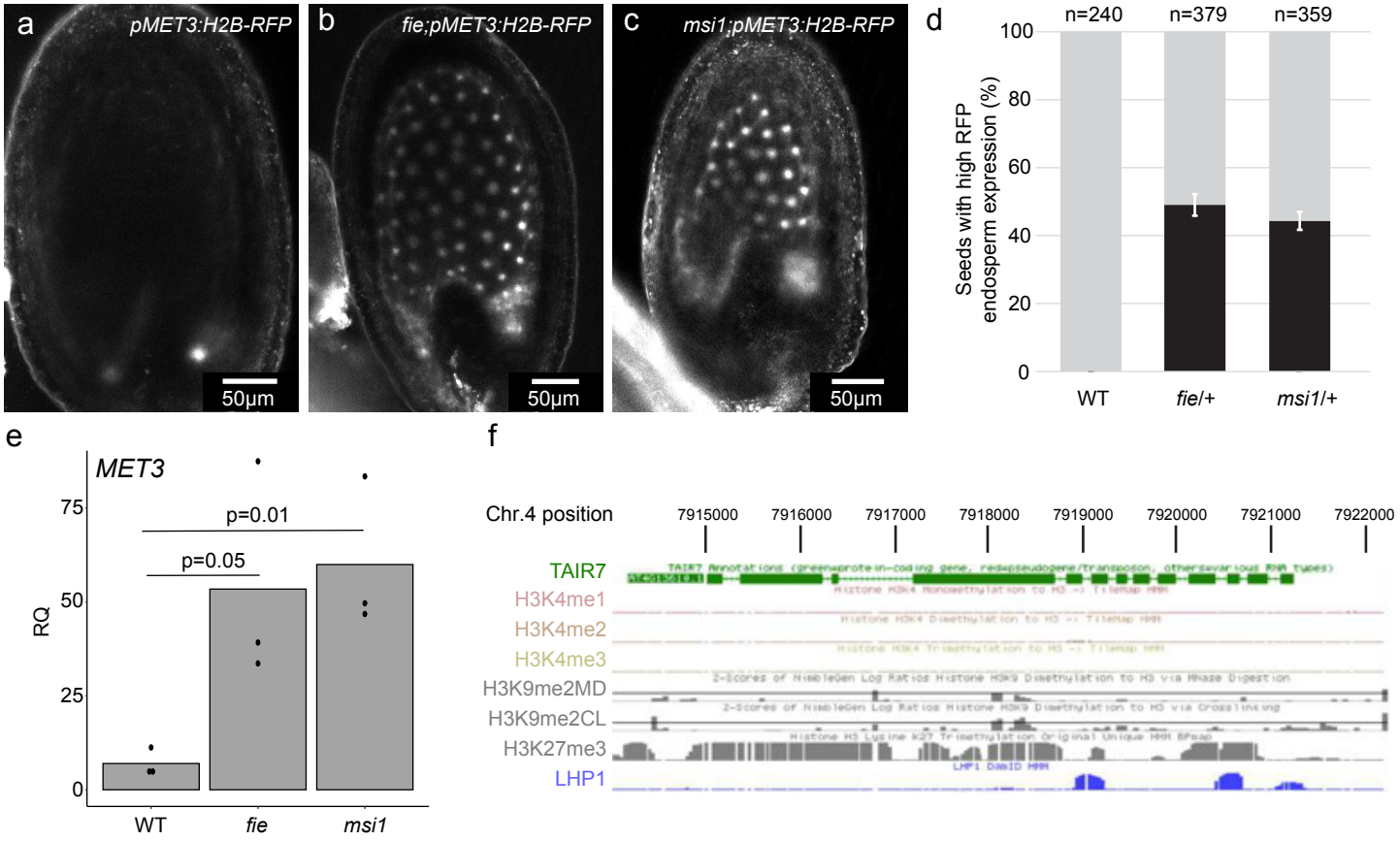

Figure 3. *MET3* expression is controlled by *FIE* and *MSI1* Polycomb proteins

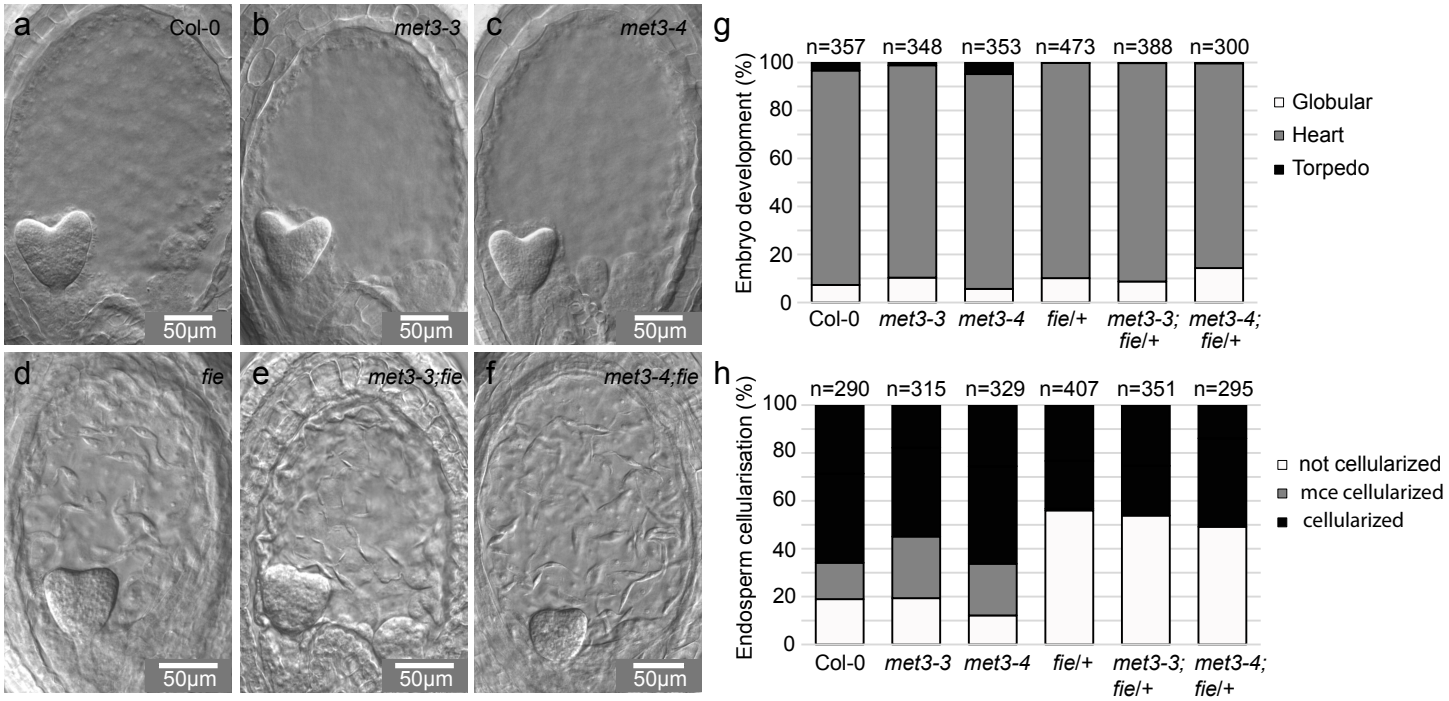

Figure 4. *MET3* does not influence *fie* phenotype

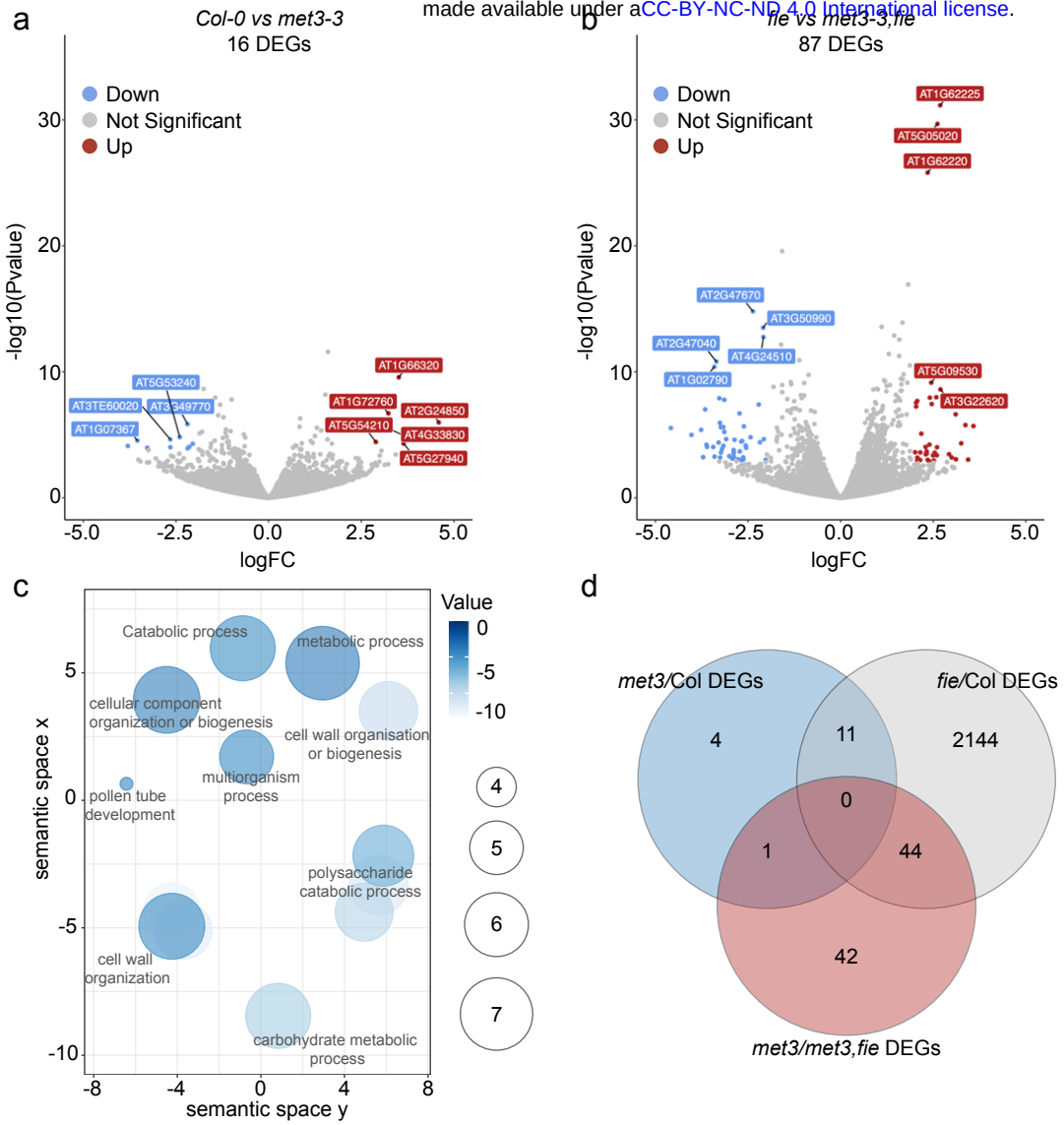

Figure 5. Transcriptome of *met3* and *met3fie* mutant seeds